

SUPPORTING INFORMATION

Silver(I) pyrophosphonates: structural, photoluminescent and thermal expansion studies

Li-Rong Guo,^a Jian-Wei Tong,^b Xu Liang,^a Jürgen Köhler,^b Jürgen Nuss,^b Yi-Zhi Li,^a

and Li-Min Zheng^{a,}*

Table S1. The lattice parameters and thermal expansion coefficients (TECs) for **4***

T / K	<i>a</i> / Å	α_a / MK ⁻¹	<i>b</i> / Å	α_b / MK ⁻¹	<i>c</i> / Å	α_c / MK ⁻¹	<i>V</i> / Å ³	α_V / MK ⁻¹
50	5.9739	37.90293	27.9860	53.70633	18.9532	46.64421	3142.103	116.85899
Error	0.0008		0.0038		0.0026		1.262	
75	5.9784	35.33134	27.9982	41.63226	18.9721	44.42306	3149.045	107.53609
Error	0.0008		0.0038		0.0026		1.265	
100	5.9852	37.90293	28.0328	43.62072	18.9973	46.64421	3161.257	119.74485
Error	0.0009		0.0044		0.0030		1.468	
125	5.9903	37.16500	28.0563	41.63226	19.0213	47.46921	3170.618	119.76886
Error	0.0009		0.0041		0.0028		1.381	
150	5.9956	36.89666	28.0838	41.26203	19.0481	49.00639	3181.012	121.98941
Error	0.0009		0.0040		0.0028		1.350	
175	6.0011	36.89666	28.1129	41.32516	19.0765	50.58789	3191.857	124.40050
Error	0.0008		0.0038		0.0026		1.287	
200	6.0087	38.65763	28.1481	42.46526	19.1065	52.19709	3204.771	129.52044
Error	0.0010		0.0047		0.0032		1.589	
225	6.0158	39.65459	28.1738	41.83926	19.1475	56.03416	3218.123	134.12578
Error	0.0010		0.0046		0.0032		1.576	
250	6.0169	36.42706	28.1999	41.39579	19.1872	58.82882	3228.236	133.66261
Error	0.0009		0.0044		0.0031		1.506	
275	6.0217	36.04285	28.2434	43.29989	19.2511	65.76920	3246.168	142.38547
Error	0.0009		0.0044		0.0031		1.517	
298	6.0241	34.61172	28.2730	43.51672	19.3138	71.82011	3261.081	147.41584
Error	0.0011		0.0049		0.0034		1.692	

* The lattice parameters are determined by X-ray single crystal diffraction over temperature range of 50-275 K and 298 K; and the thermal expansion coefficients (TECs) are calculated by equation of $\alpha_i = \partial \ln(l) / \partial T$, respectively ($M = 10^{-6}$).

Table S2. The lattice parameters and thermal expansion coefficients (TECs) for **5***

T / K	$a / \text{Å}$	$\alpha_a / \text{MK}^{-1}$	$b / \text{Å}$	$c / \text{Å}$	$\alpha_c / \text{MK}^{-1}$	$V / \text{Å}^3$	$\alpha_V / \text{MK}^{-1}$
50	5.76125	31.18763	10.79890	12.21741	37.80436	743.35	129.30305
Error	0.00068		0.00129	0.00143		0.26	
75	5.76426	27.76870	10.79677	12.22375	32.13507	744.05	98.83898
Error	0.00068		0.00129	0.00143		0.26	
100	5.77022	31.18763	10.80397	12.24046	37.80436	746.54	107.84281
Error	0.00141		0.00265	0.00295		0.54	
125	5.77409	30.33232	10.80331	12.25048	36.81702	747.70	98.83898
Error	0.00129		0.00243	0.00271		0.49	
150	5.78071	32.94925	10.80575	12.26649	39.43353	749.81	101.41150
Error	0.00119		0.00224	0.00250		0.46	
175	5.78569	33.18932	10.80934	12.28258	41.33995	751.86	102.78480
Error	0.00119		0.00225	0.00251		0.46	
200	5.79102	33.67360	10.81345	12.30646	45.96387	754.48	107.67356
Error	0.00138		0.00261	0.00292		0.53	
225	5.80432	40.20821	10.79248	12.32148	46.33107	755.84	103.89376
Error	0.00225		0.00419	0.00472		0.87	
250	5.81157	41.22887	10.79258	12.35069	51.27944	758.92	110.18515
Error	0.00270		0.00503	0.00565		1.04	
275	5.81671	40.73009	10.79914	12.43142	70.69140	765.62	133.15568
Error	0.00879		0.01641	0.01867		3.43	
300	5.81475	36.20014	10.78856	12.49532	82.26754	768.45	134.83171
Error	0.01145		0.02139	0.02441		4.48	

* The lattice parameters were determined by X-ray single crystal diffraction in the temperature range of 50-300 K; and the thermal expansion coefficients (TECs) are calculated by equation of $\alpha_l = \partial \ln(l) / \partial T$, respectively ($M = 10^{-6}$).

Table S3. Crystallographic Data and Refinement Parameters for **5** determined at 50 K and 150 K, respectively.

Compound 5	50 K	150 K
Empirical formula	C ₉ H ₆ Ag ₃ NO ₅ P ₂ S ₂	C ₉ H ₆ Ag ₃ NO ₅ P ₂ S ₂
Fw	657.82	657.82
Crystal system	Triclinic	Triclinic
Space group	<i>P</i> $\bar{1}$	<i>P</i> $\bar{1}$
<i>a</i> (Å)	5.764(1)	5.785(1)
<i>b</i> (Å)	10.801(1)	10.812(1)
<i>c</i> (Å)	12.218(1)	12.269(1)
α (°)	83.0(1)	83.0(1)
β (°)	85.9(1)	85.9(1)
γ (°)	81.0(1)	81.1(1)
<i>V</i> (Å ³)	744.4(1)	751.4(1)
<i>Z</i>	2	2
ρ_{calcd} (g·cm ⁻³)	2.935	2.908
<i>F</i> (000)	620	620
μ (Mo-K α) (mm ⁻¹)	4.420	4.380
Total, unique data, <i>R</i> _{int}	7158, 2918, 0.0219	7268, 2945, 0.0243
Observed data [<i>I</i> > 2 σ (<i>I</i>)]	2366	2379
Goodness-of-fit on <i>F</i> ²	1.046	1.152
<i>R</i> ₁ , <i>wR</i> ₂ [<i>I</i> > 2 σ (<i>I</i>)] ^a	0.0319, 0.0708	0.0335, 0.0788
<i>R</i> ₁ , <i>wR</i> ₂ (All data) ^a	0.0434, 0.0740	0.0444, 0.0816
($\Delta\rho$) _{max} , ($\Delta\rho$) _{min} /e Å ⁻³	0.835, -0.851	0.870, -0.940

^a $R_1 = \sum ||F_o| - |F_c|| / \sum |F_o|$; $wR_2 = [\sum w(F_o^2 - F_c^2)^2 / \sum w(F_o^2)]$

Table S4. Bond Lengths (Å) and Angles (°) for **5^a** Measured at 50 K and 150 K, respectively.

	50 K	150 K
Ag1-X	2.065(6)	2.059(5)
Ag1-O4	2.269(4)	2.280(4)
Ag1-O1A	2.433(4)	2.433(4)
Ag2-O1A	2.300(4)	2.303(4)
Ag2-O2	2.364(4)	2.350(4)
Ag2-O5B	2.432(4)	2.436(4)
Ag3-X'C	2.016(6)	2.010(5)
Ag3-O5	2.119(4)	2.132(4)
P1-O1	1.497(4)	1.484(4)
P1-O2	1.501(4)	1.482(4)
P1-O3	1.604(4)	1.619(4)
P2-O3	1.615(4)	1.610(4)
P2-O4	1.505(4)	1.502(4)
P2-O5	1.507(4)	1.508(4)
P1-C1	1.774(6)	1.751(5)
P2-C5	1.765(6)	1.756(5)
X-X'	1.182(9)	1.177(7)
X-Ag1-O4	160.1(2)	158.6(2)
X-Ag1-O1A	111.2(2)	112.4(2)
O4-Ag1-O1A	88.7(1)	88.9(1)
O1A-Ag2-O2	157.7(2)	156.3(1)
O1A-Ag2-O5B	118.2(1)	118.8(1)
O2-Ag2-O5B	84.1(1)	84.9(1)
X'C-Ag3-O5	171.7(2)	170.7(2)
P1-O3-P2	128.3(3)	128.3(2)
Ag2A-O1-Ag1A	84.4(1)	84.7(1)
Ag3-O5-Ag2B	87.7(1)	87.6(1)

^a Symmetry codes: A: -x + 1, -y + 2, -z; B: -x + 2, -y + 2, -z; C: -x + 2, -y + 3, -z; D: x - 1, y, z; E: x + 1, y, z; F: -x + 1, -y + 3, -z.

Table S5. Comparison of Selected Bond Lengths (Å) and Angles (°) for **5^a** at 50 K and 150 K

	50 K	150 K
Ag1-Ag2	3.181(1)	3.191(1)
Ag2-Ag3B	3.161(1)	3.170(1)
Ag1-Ag3	3.099(1)	3.105(1)
Ag1-Ag3D	3.372(1)	3.379(1)
Ag2-Ag2A	3.166(1)	3.192(1)
Ag1-X	2.065(6)	2.059(5)
Ag3-X'C	2.016(6)	2.010(5)
X-X'	1.182(9)	1.177(7)
Ag1-Ag3B	6.329(1)	6.347(1)
Ag1-Ag3C	5.253(1)	5.240(1)
Ag2-Ag1-Ag3	97.2(1)	97.1(1)
Ag1-Ag2-Ag3B	172.5(1)	172.4(1)
Ag1-Ag3-Ag2B	90.2(1)	90.4(1)
Ag3B-Ag2-Ag2A	101.4(1)	101.4(1)
Ag2-Ag2A-Ag1A	82.1(1)	81.6(1)
Ag2-Ag1-Ag3D	96.6(1)	97.1(1)
Ag1A-Ag3B-Ag2	79.2(1)	79.1(1)
Ag1-X-X'	171.9(5)	173.9(5)
X-X'-Ag3C	175.3(5)	175.6(4)
X-Ag1-Ag3	81.2(2)	80.4(2)
X'C-Ag3-Ag1	102.6(2)	103.7(1)
X-Ag1-Ag3D	120.8(2)	120.4(2)
X'-Ag3C-Ag1F	59.6(2)	59.7(1)

^a Symmetry codes: A: -x + 1, -y + 2, -z; B: -x + 2, -y + 2, -z; C: -x + 2, -y + 3, -z; D: x - 1, y, z; E: x + 1, y, z; F: -x + 1, -y + 3, -z.

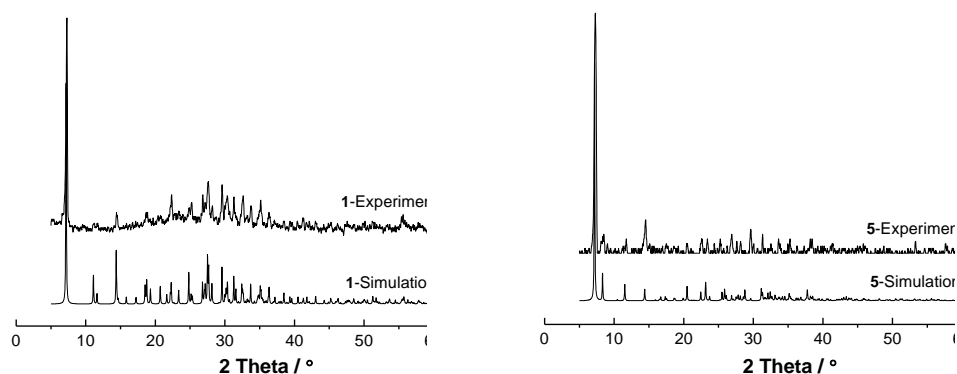


Figure S1. PXRD patterns derived from single crystal data and recorded by experiments for **1** (left) and **5** (right).

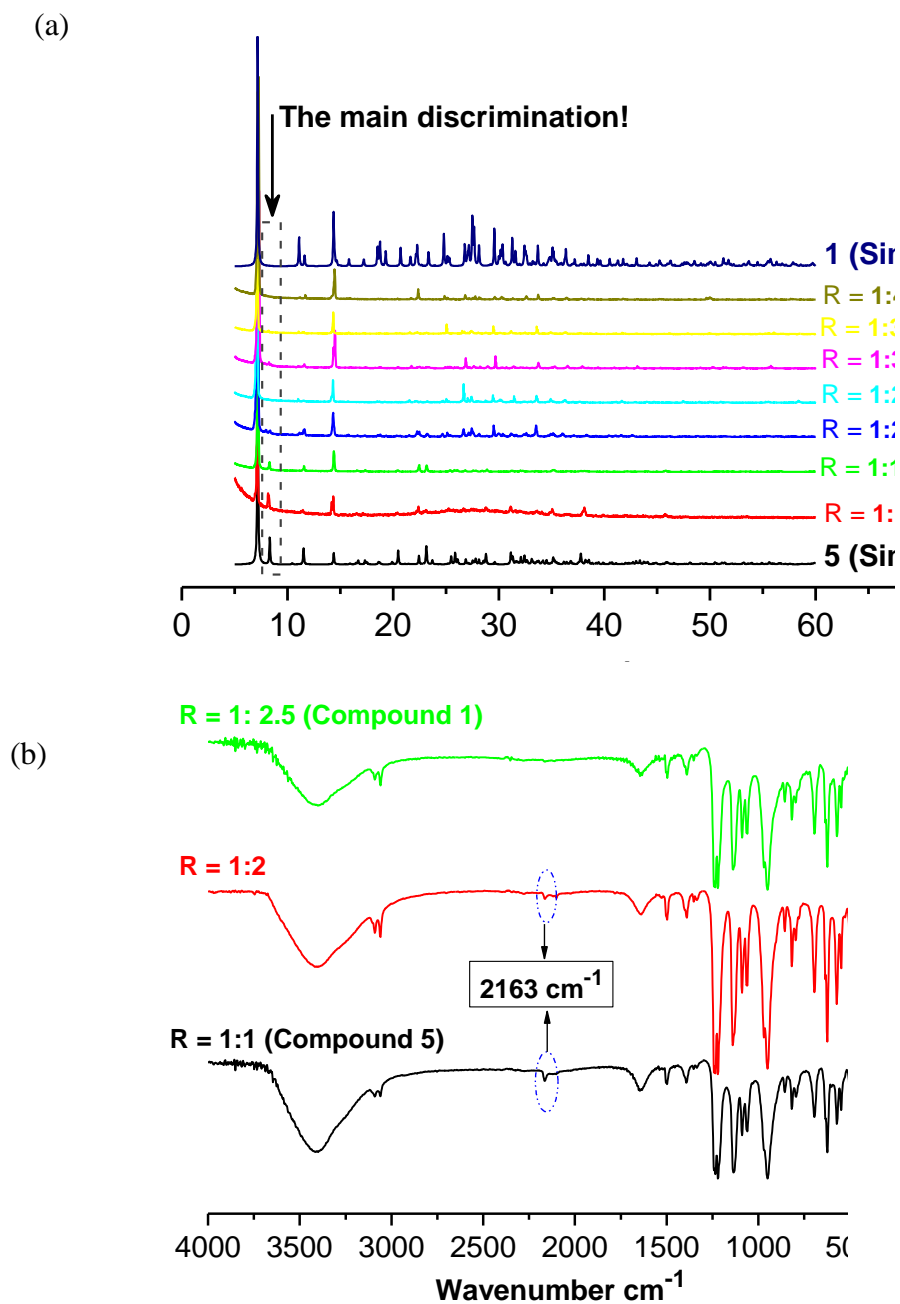


Figure S2. PXR patterns (a) and IR spectra (b) carried out on crystalline products of reacting 3-TPA with AgNO₃ in different molar ratio in acetonitrile at 120°C for 48 hours. R is the molar ratio of 3-TPA to AgNO₃. **1** (Simul.) and **5** (Simul.) represent the XRD patterns simulated from single crystal structures of **1** and **5**, respectively.

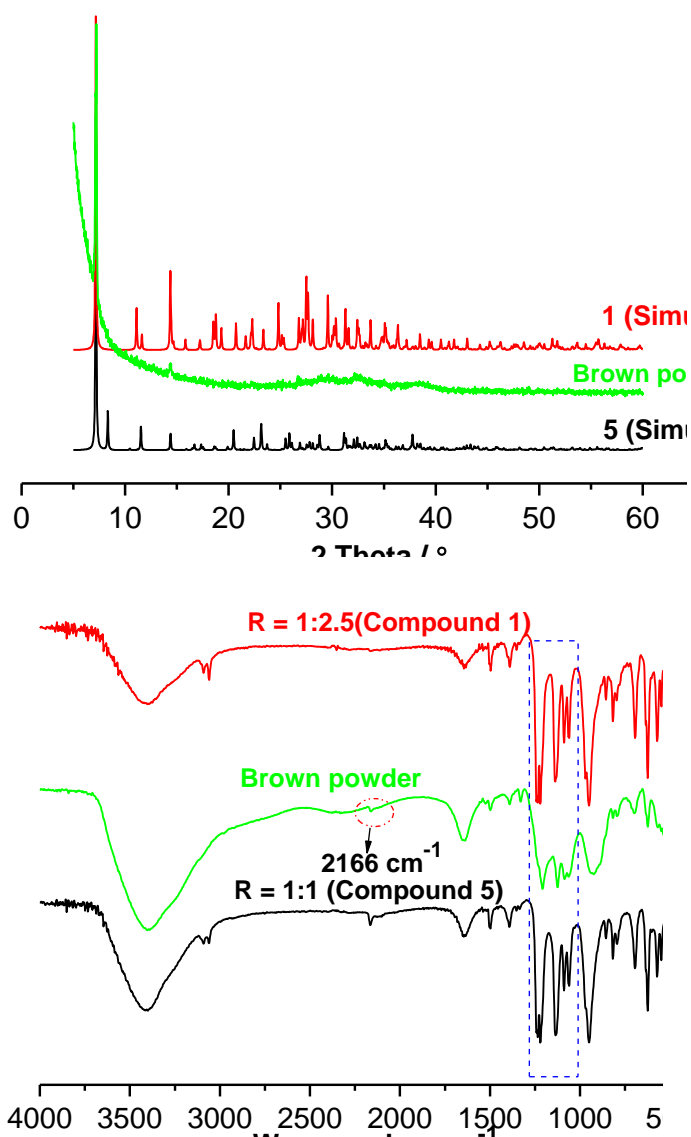


Figure S3. PXRD patterns (a) and IR Spectrum (b) carried out on brown powders which are byproducts by reacting 3-TPA with AgNO_3 in the range of $R = 1:2.5$ to $1:4$ in acetonitrile for 48 hours. For comparison, the XRD patterns simulated from compounds **1** and **5**, as well as the IR spectra of **1** and **5** are presented.

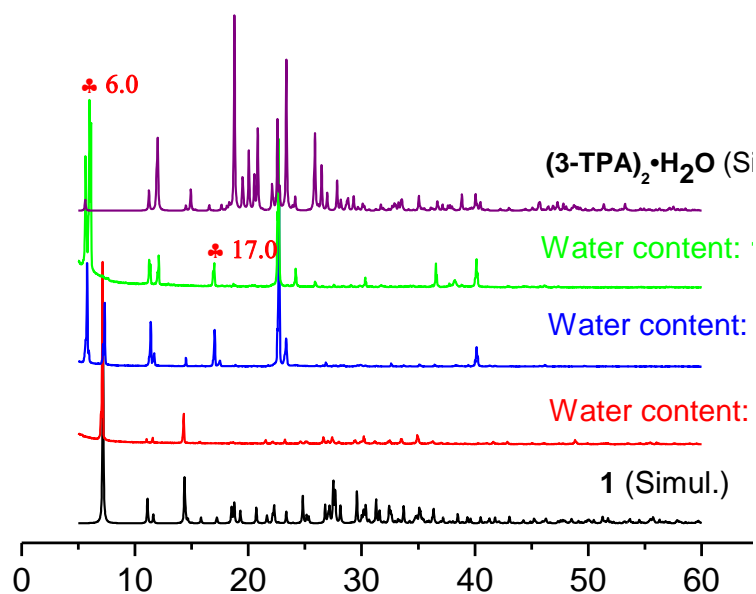


Figure S4. PXRD patterns carried out on solid products by reacting 3-TPA with AgNO_3 in molar ratio of 1:2.5 in acetonitrile with different water contents at 120°C for 48 hours. **1** (Simul.) and $(3\text{-TPA})_2\cdot\text{H}_2\text{O}$ (Simul.) represent the XRD patterns simulated from compounds **1** and $(3\text{-TPA})_2\cdot\text{H}_2\text{O}$, respectively. The peaks at $2\theta = 6.0^\circ$ and 17.0° in the PXRD pattern of “water content: 10.20%” come from an unrecognized black powder.

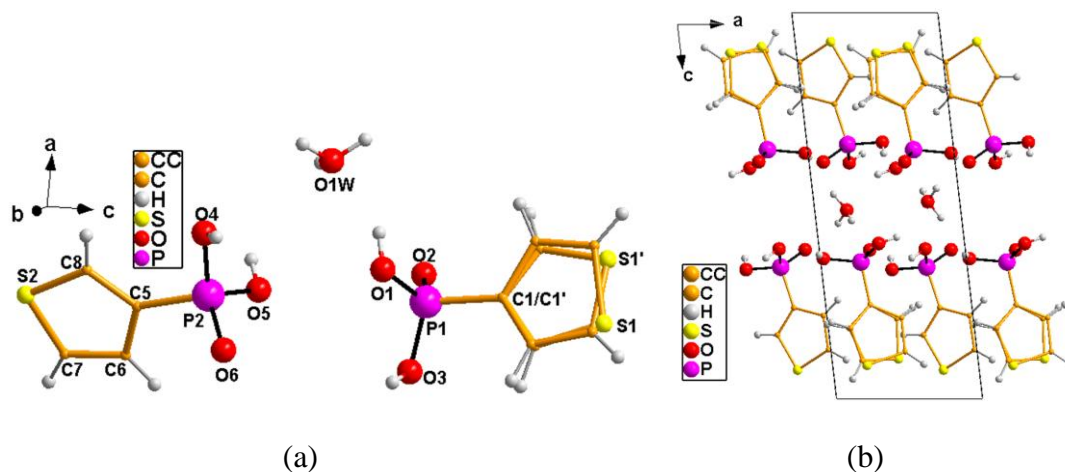
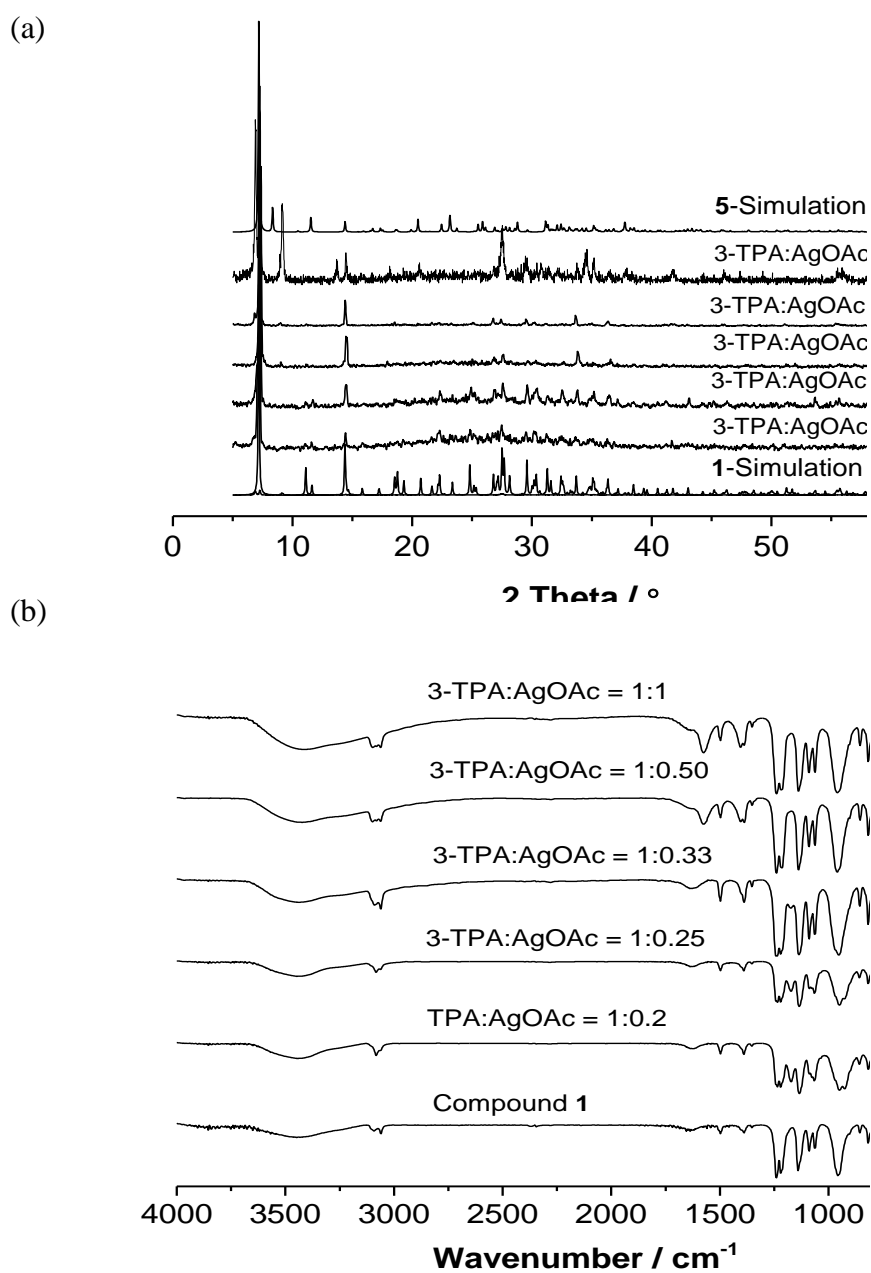


Figure S5. (a) The crystallographic unit of compound $(3\text{-TPA})_2\cdot\text{H}_2\text{O}$, one of the thienyl groups and one hydrogen atom connected with O1W are disordered; (b) The packing diagram of $(3\text{-TPA})_2\cdot\text{H}_2\text{O}$ along *b*-axis. Selected bond lengths: C1-P1 1.792(5), P1-O1 1.525(3), P1-O2 1.493(3), P1-O3 1.549(3), C5-P2 1.773(6), P2-O4 1.530(3), P2-O5 1.563(3), P2-O6 1.491(4) Å.



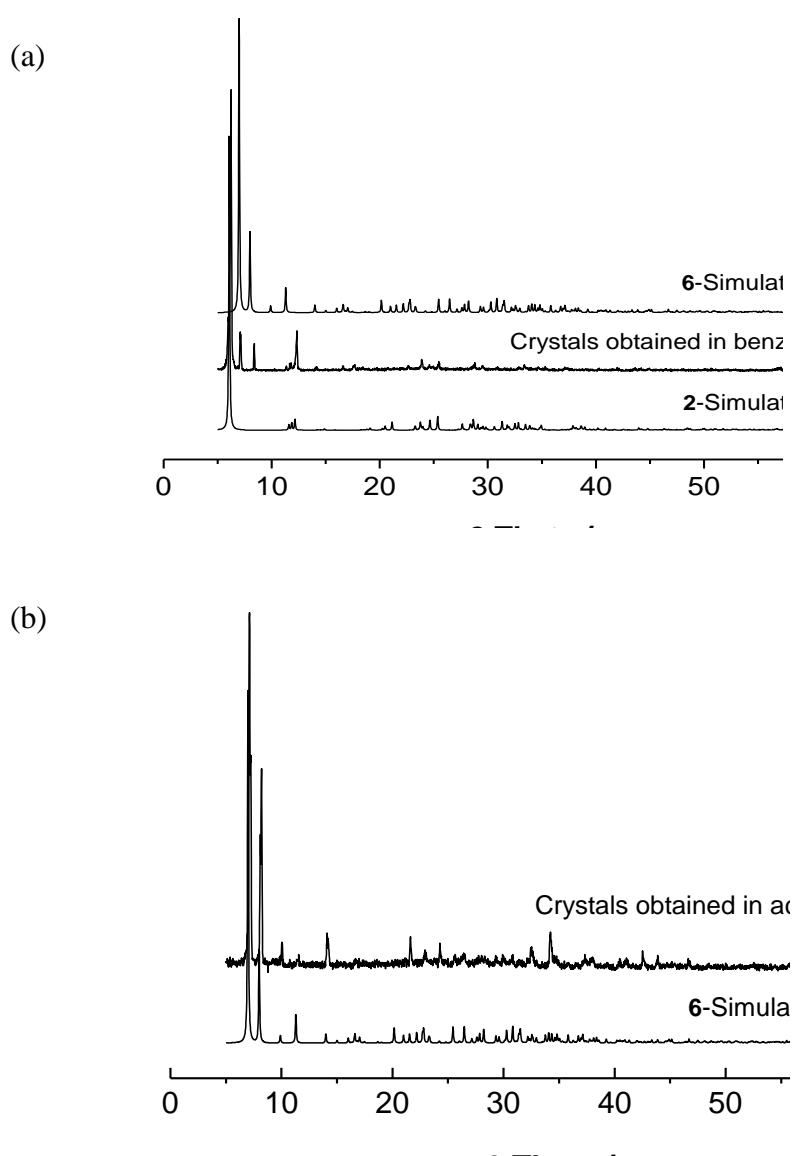


Figure S7. PXRD patterns recorded on crystals obtained in benzonitrile (a) and acetonitrile (b). The PXRD patterns derived from single crystal data of compounds **2** and **6** are also presented.

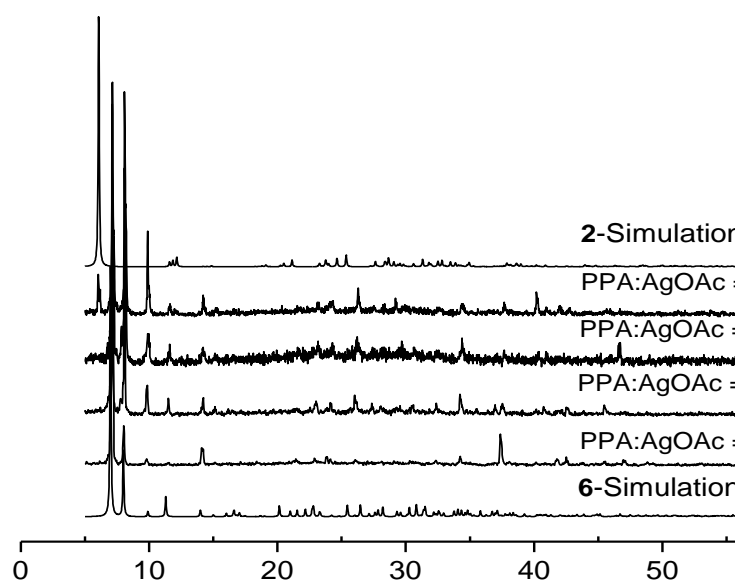


Figure S8. PXRD patterns recorded on solid products by reacting PPA with AgOAc in the molar ratio of 1:0.25-1 in A. R. MeCN at 120 °C for 3 days ($C_{\text{AgOAc}} = 0.0154 \text{ mol}\cdot\text{L}^{-1}$). PXRD patterns simulated from structures **2** and **6** are also presented.

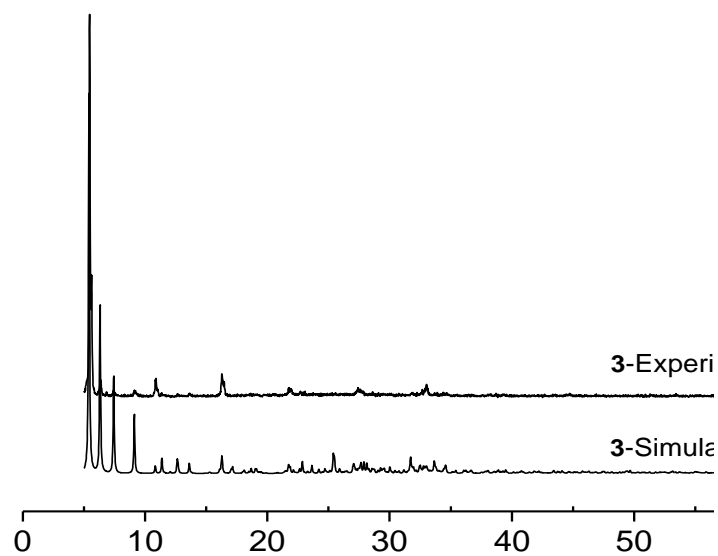


Figure S9. PXRD pattern of compound **3** and that simulated from single crystal data of **3**.

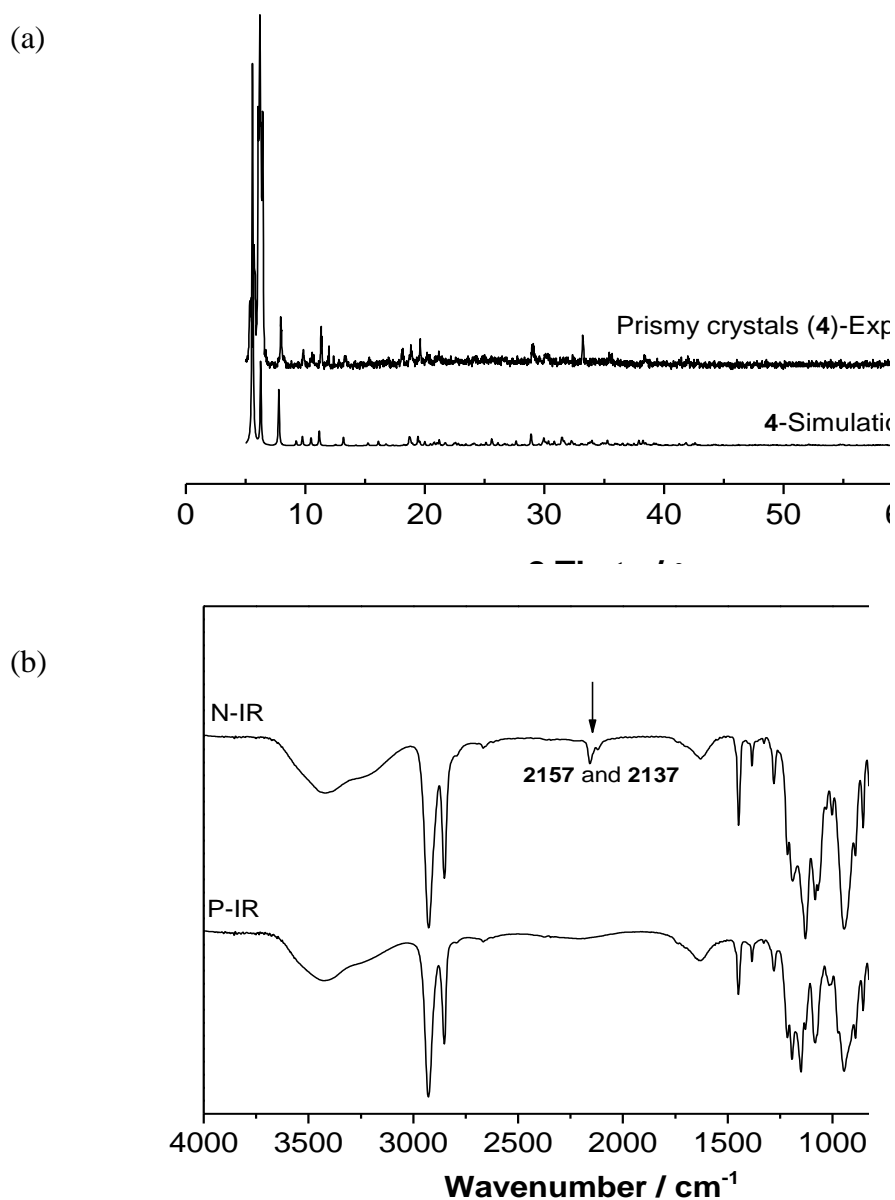


Figure S10. (a) PXR D patterns simulated and experimented from prismatic crystals of **4**. (b) IR spectra of prism shaped (P-IR) and needle-shaped (N-IR) crystals.

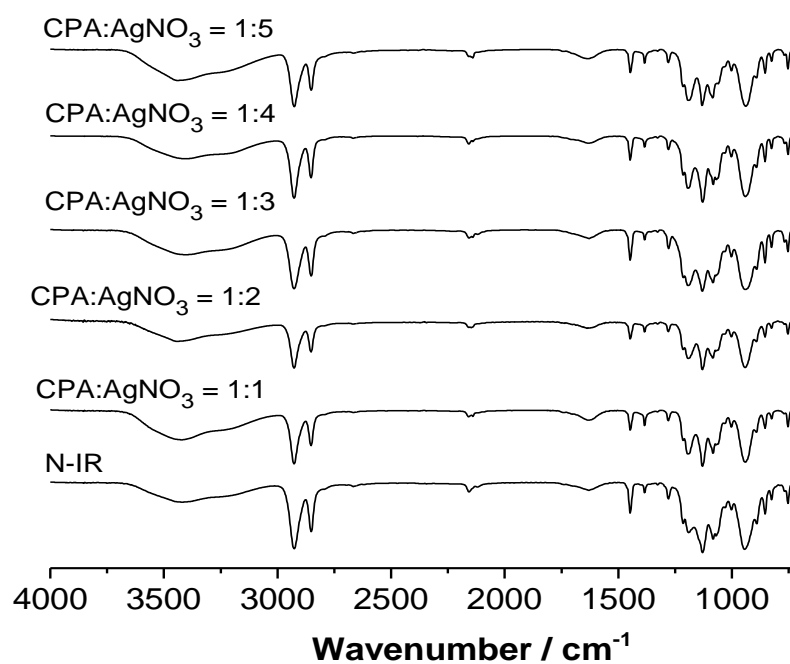


Figure S11. IR spectra of solid products obtained by reacting CPA with AgNO₃ with the molar ratio from 1:1 to 1:5 in A. R. MeCN at 120 °C for 3 days ($C_{\text{CPA}} = 0.0308 \text{ mol}\cdot\text{L}^{-1}$). The IR spectrum of needle product is denoted as N-IR.

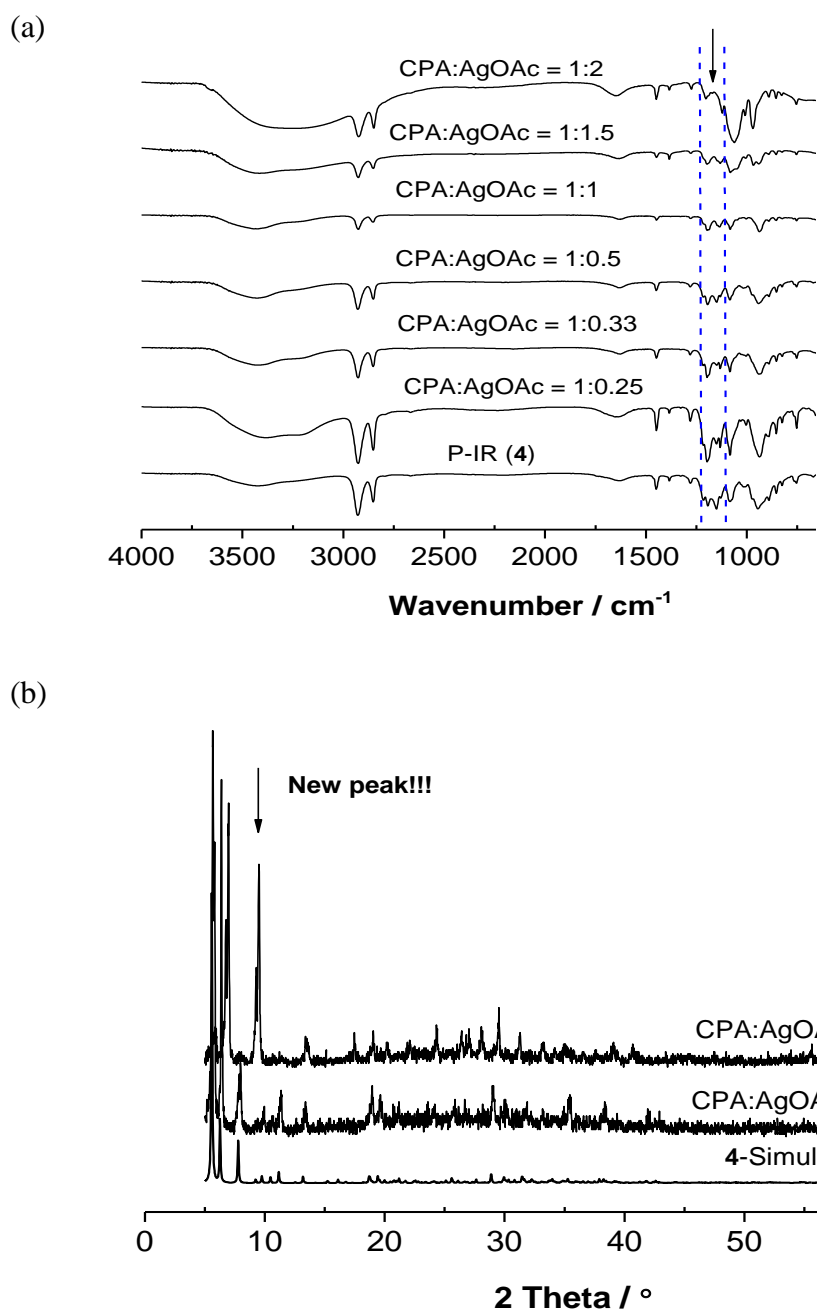


Figure S12. (a) IR spectra of solid products by reacting CPA with AgOAc in A. R. MeCN with the molar ratio of 1:0.25-2 at 120 °C for 3 days. The IR spectrum of prism product (**4**) is denoted as P-IR. (b) PXRD patterns on solid products by reacting CPA with AgOAc with the molar ratio of 1:0.5-1 ($C_{\text{AgOAc}} = 0.0154 \text{ mol}\cdot\text{L}^{-1}$). The IR spectra show that the major product is **4** and the cyanide phase disappeared. The subtle changes within the range of 1216-1130 cm^{-1} in the IR spectra of 1:1-2 and the emergence of new peak in the XRD pattern in the molar ratio of 1:1 suggest a new substance is generated together with **4** over this range.

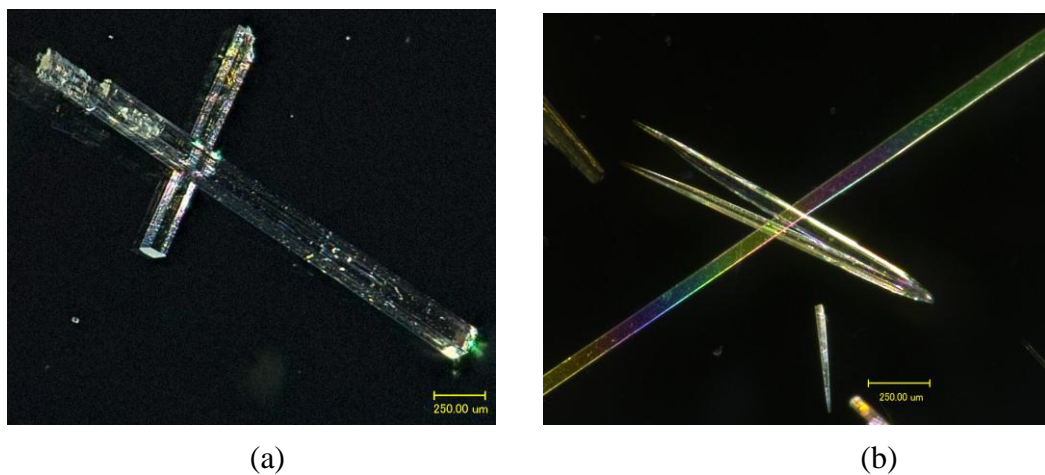


Figure S13. The crystal figurations of compounds **4** (a) and **5** (b) for thermal expansion measurements.

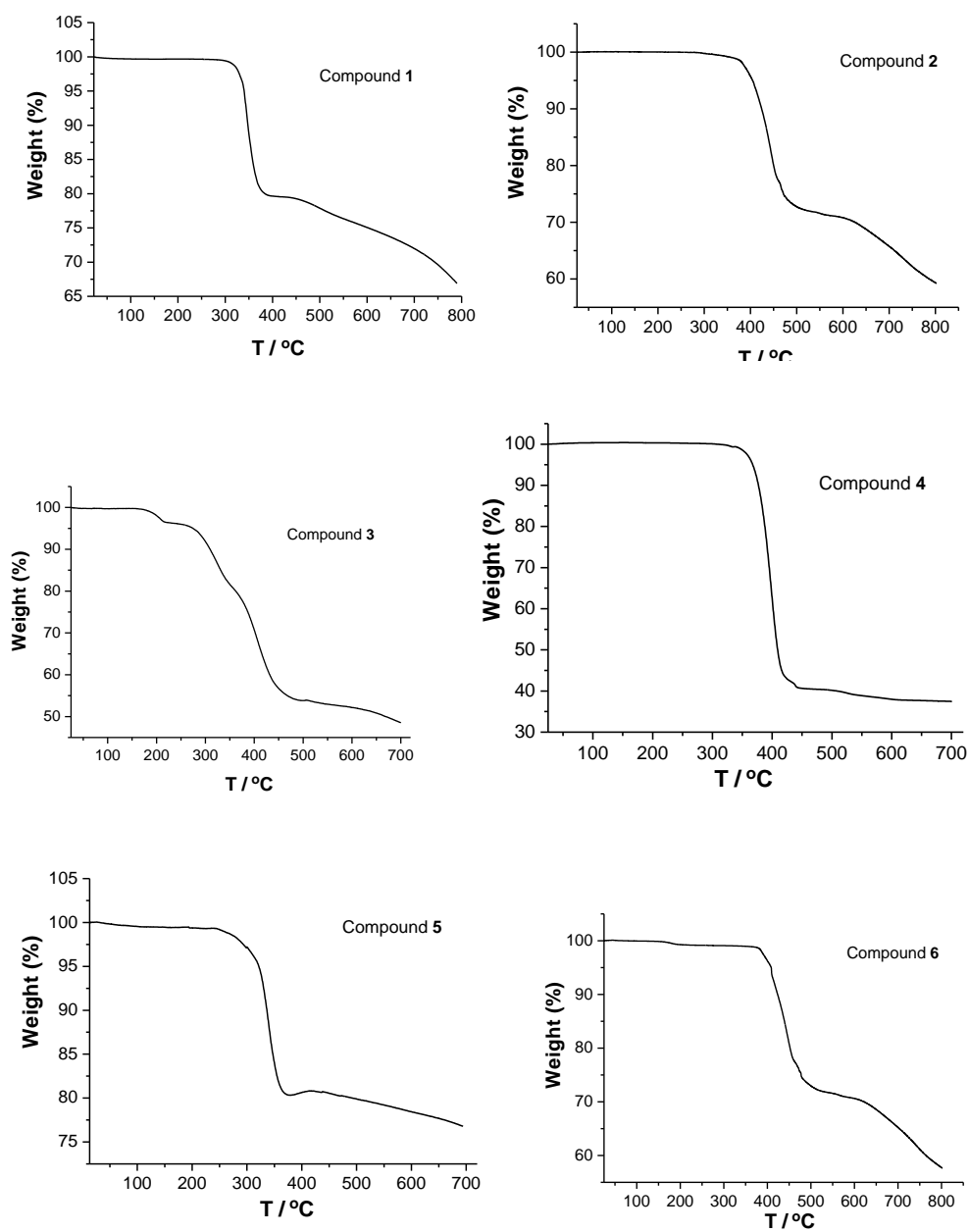


Figure S14. Thermal analyses of compounds 1-6.